

Selective Transfer of Rotationally Commensurate MoS from an Epitaxially Grown van der Waals Heterostructure

Junmo Kang, Itamar Balla, Xiaolong Liu, Hadallia Bergeron,
Soo Kim, Christopher Wolverton, and Mark C Hersam

Chem. Mater., **Just Accepted Manuscript** • DOI: 10.1021/acs.chemmater.8b03128 • Publication Date (Web): 16 Nov 2018

Downloaded from <http://pubs.acs.org> on November 21, 2018

Just Accepted

“Just Accepted” manuscripts have been peer-reviewed and accepted for publication. They are posted online prior to technical editing, formatting for publication and author proofing. The American Chemical Society provides “Just Accepted” as a service to the research community to expedite the dissemination of scientific material as soon as possible after acceptance. “Just Accepted” manuscripts appear in full in PDF format accompanied by an HTML abstract. “Just Accepted” manuscripts have been fully peer reviewed, but should not be considered the official version of record. They are citable by the Digital Object Identifier (DOI®). “Just Accepted” is an optional service offered to authors. Therefore, the “Just Accepted” Web site may not include all articles that will be published in the journal. After a manuscript is technically edited and formatted, it will be removed from the “Just Accepted” Web site and published as an ASAP article. Note that technical editing may introduce minor changes to the manuscript text and/or graphics which could affect content, and all legal disclaimers and ethical guidelines that apply to the journal pertain. ACS cannot be held responsible for errors or consequences arising from the use of information contained in these “Just Accepted” manuscripts.



Selective Transfer of Rotationally Commensurate MoS₂ from an Epitaxially Grown van der Waals Heterostructure

Junmo Kang^{1,‡}, Itamar Balla^{1,‡}, Xiaolong Liu², Hadallia Bergeron¹, Soo Kim^{1,†}, Christopher Wolverton¹, and Mark C. Hersam^{1,2,3,4,*}

¹Department of Materials Science and Engineering, Northwestern University, Evanston, Illinois 60208, United States

²Applied Physics Graduate Program, Northwestern University, Evanston, Illinois 60208, United States

³Department of Chemistry, Northwestern University, Evanston, Illinois 60208, United States

⁴Department of Electrical Engineering and Computer Science, Northwestern University, Evanston, Illinois 60208, United States

‡Authors with equal contribution

ABSTRACT: Large-scale synthesis of high quality two-dimensional (2D) semiconductors are critical for their incorporation in emerging electronic and optoelectronic technologies. In particular, chemical vapor deposition (CVD) of transition metal dichalcogenides (TMDs) *via* van der Waals epitaxy on epitaxial graphene (EG) leads to rotationally commensurate TMDs in contrast to randomly aligned TMDs grown on amorphous oxide substrates. However, the interlayer coupling between TMDs and EG hinders the investigation and utilization of the intrinsic electronic properties of the resulting TMDs, thus requiring their isolation from the EG growth substrate. To address this issue, we report here a technique for selectively transferring monolayer molybdenum disulfide (MoS₂) from CVD-grown MoS₂-EG van der Waals heterojunctions using copper (Cu) adhesion layers. The choice of Cu as the adhesion layer is motivated by density functional theory calculations that predict the preferential binding of monolayer MoS₂ to Cu in contrast to graphene. Atomic force microscopy and optical spectroscopy confirm the large-scale transfer of rotationally commensurate MoS₂ onto SiO₂/Si substrates without cracks, wrinkles, or residues. Furthermore, the transferred MoS₂ shows high performance in field-effect transistors with mobilities up to 30 cm²/Vs and on/off ratios up to 10⁶ at room temperature. This transfer technique can likely be generalized to other TMDs and related 2D materials grown on EG, thus offering a broad range of benefits in nanoelectronic, optoelectronic, and photonic applications.

INTRODUCTION Two-dimensional (2D) transition metal dichalcogenides (TMDs) are layered materials with a diverse range of desirable electronic, optical, and mechanical properties.¹⁻⁵ In particular, monolayer molybdenum disulfide (MoS₂) is a direct band gap semiconductor with broad potential for optoelectronic applications.⁶⁻⁸ While monolayer MoS₂ can be synthesized at wafer scales *via* chemical vapor deposition (CVD),⁹⁻¹² the quality and crystallographic orientation of CVD MoS₂ strongly depends on the choice of substrate. For example, when amorphous SiO₂ and high-κ dielectrics are used as growth substrates, the MoS₂ domains are randomly oriented,^{10,13} resulting in a high concentration of grain boundaries that degrade the electrical and mechanical properties of monolayer films.¹⁴⁻¹⁷ In contrast, the ordering of crystalline substrates can template rotationally commensurate van der Waals epitaxy, leading to reduced defect density and suppression of tilt grain boundary formation.¹⁸⁻²⁰ A particularly narrow azimuthal distribution of MoS₂ grains across large areas has been observed for CVD-grown MoS₂ on epitaxial graphene (EG) on SiC substrates.¹⁹

However, due to the presence of the underlying semi-metallic graphene, the resulting MoS₂-EG heterostructure hinders fundamental charge transport studies and electronic devices of the as-grown MoS₂. Therefore, it is necessary to develop a reliable technique to transfer MoS₂ from EG onto dielectric substrates without compromising electronic properties.

Previous work has successfully transferred 2D materials from growth substrates using wet-transfer techniques based on polymer supports.^{14,21,22} However, wet-transfer methods suffer from polymeric residues and wrinkles on the transferred TMD thin films, which significantly degrade the performance of TMD-based devices.^{23,24} Alternatively, recent 2D material transfer methods have explored the physical delamination of TMDs from growth substrates mediated by metal adhesion layers.²⁵⁻²⁷ While this method has shown promise in select cases, a suitable metal adhesion layer that selectively transfers TMDs from van der Waals heterostructures with EG has not yet been identified or demonstrated.

Here, we report a dry transfer method using thermal release tape (TRT) and copper (Cu) adhesion layers that selectively delaminates rotationally ordered isolated MoS₂ domains from the EG growth substrate. The choice of Cu as the adhesion layer is based on the higher binding energy of MoS₂ to Cu compared to graphene as revealed by density functional theory (DFT) calculations. The structure and properties of the transferred MoS₂ are investigated with a comprehensive suite of characterization tools including atomic force microscopy (AFM), scanning electron microscopy (SEM), transmission electron microscopy (TEM), X-ray photoelectron spectroscopy (XPS), Raman spectroscopy, and photoluminescence (PL) spectroscopy. In addition, charge transport measurements confirm that the transferred MoS₂ possesses superlative optical and electronic properties with high potential for optoelectronic applications.

RESULTS AND DISCUSSION To enable selective transfer of MoS₂ directly from the underlying EG growth substrate, it is critical to select a metal adhesion layer with strong adhesion to MoS₂ and weak adhesion to graphene. Previously reported theoretical studies suggested that silver (Ag), gold (Au), and Cu weakly adhere to graphene. However, Au has a weak binding energy to MoS₂, while the removal of Ag requires etchants that lead to the degradation of MoS₂ electronic properties by chemical doping.^{28,29} Consequently, we performed first-principles DFT calculations to determine the binding energy of Cu to MoS₂ compared to graphene. Specifically, the *opt*-type van der Waals density functional (vdW-DF) was used in an effort to account for dispersion interactions in the layered structures investigated in this work (*i.e.*, Cu, MoS₂, and graphene).^{30,31} This vdW-DF method is particularly effective in obtaining accurate structural parameters, such as the interlayer spacing in van der Waals materials.³²⁻³⁵ The DFT calculated binding energies

(E_b) for three different heterostructure systems (*i.e.*, Cu/MoS₂, Cu/graphene, and MoS₂/graphene) are summarized in **Table 1**. These theoretical results show that the binding energy is $\sim 50\%$ larger for Cu/MoS₂ compared to the Cu/graphene or MoS₂/graphene. The electron density difference isosurface plots in **Figure 1** further corroborate that the interaction between Cu and MoS₂ is the most favorable case, thus suggesting Cu as a leading adhesion layer candidate for the selective transfer of MoS₂ from MoS₂-EG van der Waals heterojunctions.

Table 1. The calculated DFT binding energy and the layer spacing.

Interfaces	E_b [meV/Å ²]	Layer Spacing [Å]
Cu/MoS ₂	-32.2	2.042
Cu/graphene	-21.9	3.030
MoS ₂ /graphene	-21.1	3.318

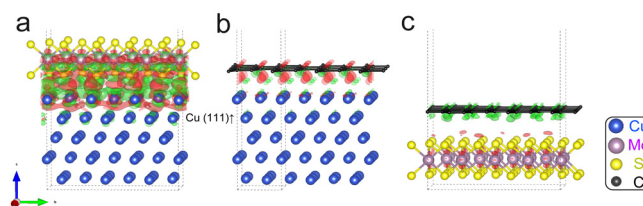


Figure 1. The electron density difference isosurface plot for: (a) Cu and MoS₂, (b) Cu and graphene, and (c) MoS₂ and graphene interfaces. The red and green regions correspond to electron accumulation and depletion regions, respectively (*i.e.*, $\pm 0.0005 e \cdot \text{\AA}^3$). The blue, purple, yellow, and black circles represent Cu, Mo, S, and C atoms, respectively.

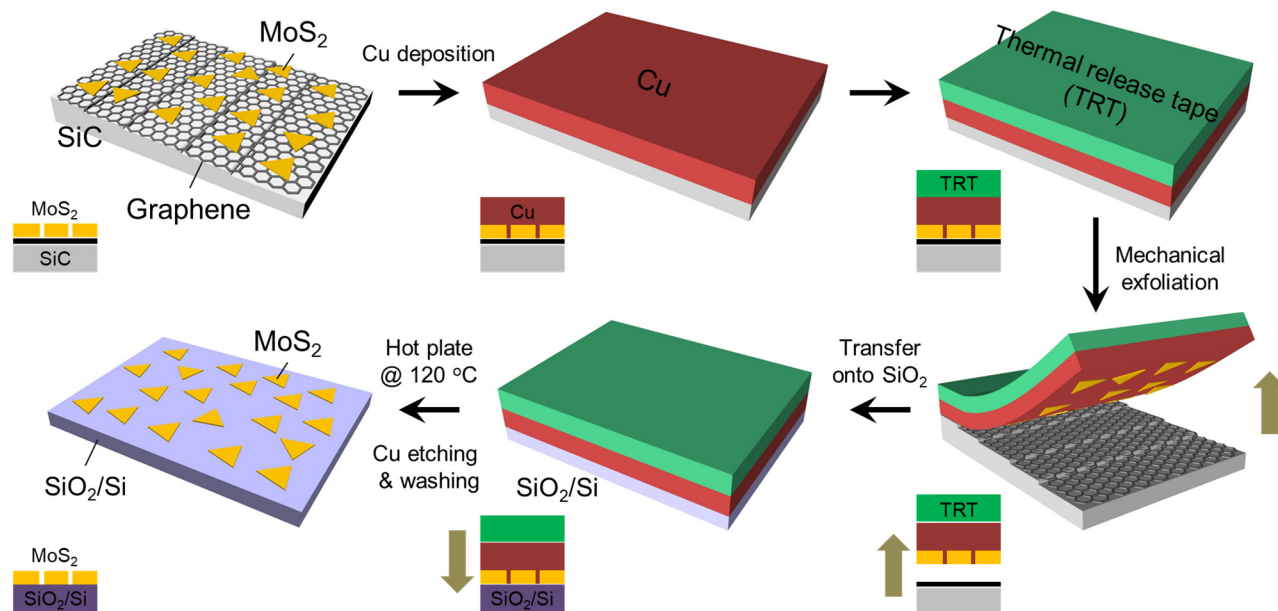


Figure 2. Schematic for the transfer process of CVD MoS₂ from EG/SiC to SiO₂/Si.

Figure 2 schematically illustrates the transfer process for CVD MoS₂ from the EG/SiC growth substrate to a SiO₂/Si substrate. The CVD growth of MoS₂ on EG/SiC was described previously.¹⁹ A 200 nm thick Cu layer is then deposited by electron-beam evaporation. The first 10 nm were deposited at a rate of 0.1 Å/s, and the remaining 190 nm were deposited at a rate of 0.5 Å/s. Next, TRT is placed on the Cu/MoS₂/EG/SiC substrate, and the stacked layer of TRT/Cu/MoS₂ is mechanically peeled off from the EG/SiC substrate. In parallel, the 300 nm thick SiO₂/Si substrate is cleaned with an O₂ plasma after which the TRT/Cu/MoS₂ stack is placed on top. The TRT is then removed while heating the SiO₂/Si substrate to 120 °C. Following TRT removal, the Cu layer is etched with a 0.01 M ammonium persulfate (APS) solution, leaving behind MoS₂ on the SiO₂/Si substrate. Finally, the MoS₂/SiO₂/Si is rinsed with DI water to remove APS solution residue.

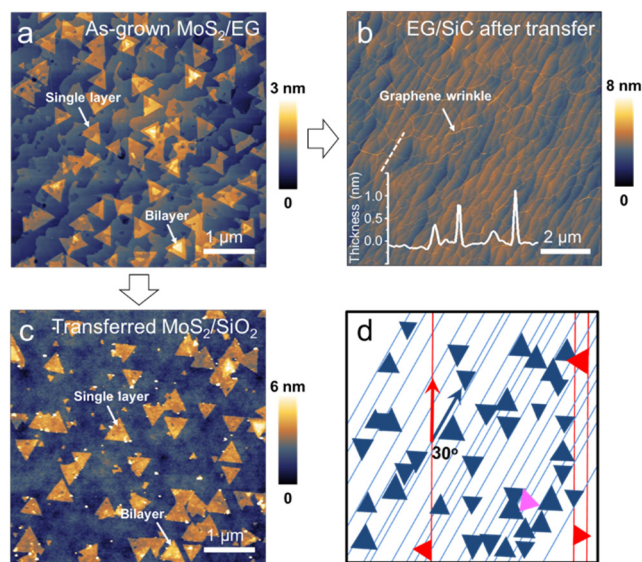


Figure 3. Transfer of CVD MoS₂ from EG/SiC to SiO₂/Si. (a-c) AFM height images of (a) as-grown MoS₂/EG, (b) EG/SiC after transfer, and (c) transferred MoS₂/SiO₂. (d) Color labeling of the crystallographic orientations of the MoS₂ flakes in (c). The majority of the MoS₂ flakes remain in rotational registry (colored blue) with a minority population rotated by 30° (colored red) and a rare randomly oriented flake (colored pink).

The surface morphology of the MoS₂ crystals before and after transfer are characterized by AFM as shown in **Figure 3**. In particular, rotationally commensurate MoS₂ domains grown on the EG/SiC substrate are shown in **Figure 3a**. Single-crystal MoS₂ triangular-shaped flakes can be clearly resolved from the AFM image and show well-defined edges with lateral sizes of ~300 - 500 nm. The MoS₂ preferentially grows at the step edges of the EG with the vast majority of the flakes being monolayer. It should be noted that ~86% of the MoS₂ flakes have their armchair direction aligned with the armchair direction of the EG across the entire EG/SiC substrate, consistent with previously reported results for CVD growth of MoS₂ on EG/SiC.¹⁹ **Figure 3b** shows the surface morphology of the EG/SiC substrate after the transfer. Compared to as-grown EG/SiC (**Figure S1a**), the morphology of EG/SiC following transfer does not change signifi-

cantly with the exception of an increase in the density of inhomogeneous wrinkles in the EG layer. The inset of **Figure 3b** shows the height profile of the graphene wrinkles to be ~1 nm, which is similar to the previously reported height of graphene wrinkles on SiO₂/Si substrates.³⁶ Raman spectroscopy was further employed to characterize the EG following transfer in comparison to the as-grown EG (**Figure S1b**). In both Raman spectra, the G band of graphene overlaps with the strong intensity peaks from the SiC substrate in addition to a 2D band at ~2680 cm⁻¹.³⁷ The 2D band of EG/SiC following transfer is red-shifted compared to as-grown EG/SiC, which suggests that tensile strain is induced in the EG when peeling off the Cu/MoS₂ layer.^{38, 39} We further note the absence of the two characteristic bands of MoS₂ (A_{1g} and E_{12g}) on the EG/SiC substrate following transfer.

An AFM image of MoS₂ flakes after transfer onto the SiO₂/Si substrate is shown in **Figure 3c**. The micrograph exhibits a flat and uniform surface for the MoS₂ domains without cracks or wrinkles. The Cu layer serves as a barrier between the MoS₂ surface and adhesive TRT residues, and then is successfully etched without mechanical damage to the MoS₂ flakes. The transfer process is effective not only for isolated MoS₂ flakes but also merged MoS₂ domains with larger lateral sizes, as well as occasional multilayer regions (**Figure S2**). **Figure 3d** depicts the crystallographic orientations of the MoS₂ flakes by plotting a line along one edge of each triangle. The majority of the triangles remain aligned (blue) with a minority population rotated by 30° (red) and a rare randomly oriented flake (pink). This approach thus allows the rotational ordering of MoS₂ flakes grown on EG to be transferred to other substrates including amorphous SiO₂.

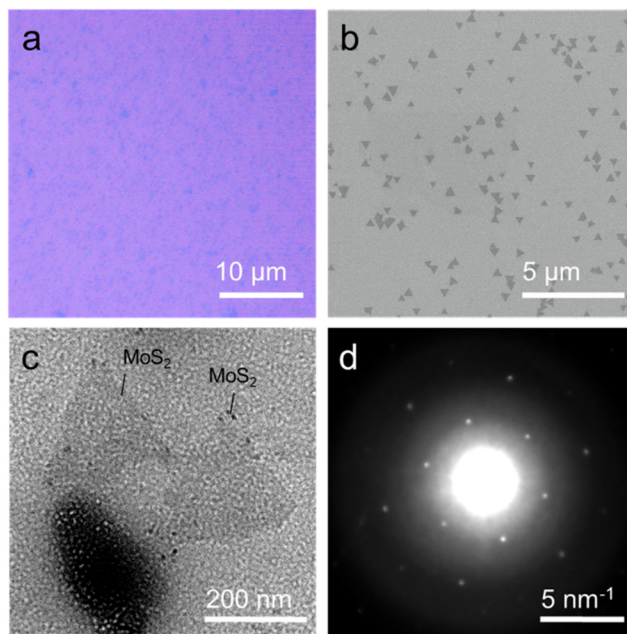


Figure 4. Structural characteristics of transferred MoS₂. (a) Optical image of transferred MoS₂ on SiO₂. (b) SEM image of transferred MoS₂ on SiO₂. (c) TEM image of transferred MoS₂ crystals on a TEM grid. (d) SAED pattern taken on a monolayer MoS₂ crystal, which shows clear diffraction spots.

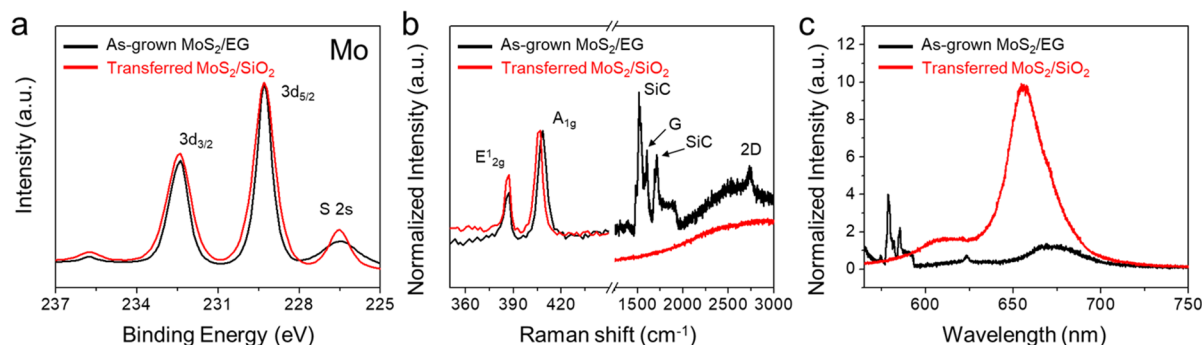


Figure 5. Spectroscopic characterization of transferred MoS₂. (a) XPS, (b) Raman, and (c) PL spectra of as-grown MoS₂/EG and transferred MoS₂/SiO₂. The Raman and PL intensities are normalized to the Raman A1g peak.

The structural characteristics of the transferred MoS₂ flakes are further investigated by optical and electron microscopy in **Figure 4**. **Figure 4a** presents an optical image of the transferred MoS₂/SiO₂ substrate, showing spatial uniformity over relatively large areas. An SEM image of the transferred MoS₂/SiO₂ substrate is shown in **Figure 4b**, confirming that the MoS₂ crystals are transferred without detectable residues. Furthermore, the transferred MoS₂ flakes are characterized by TEM in **Figure 4c**. The TEM image shows triangular MoS₂ crystals with aligned edge orientations, which is consistent with the earlier AFM images. The high crystallinity of the transferred MoS₂ flakes is confirmed by selected area electron diffraction (SAED) in **Figure 4d**. The SAED reveals a hexagonal diffraction pattern, which is indicative of a highly crystalline MoS₂ sample with minimal structural distortion induced during transfer.^{9,40}

In order to confirm that the transfer process does not strongly influence the chemical integrity of MoS₂, spectroscopic characterization was performed on as-grown MoS₂/EG and transferred MoS₂/SiO₂ (**Figure 5**). XPS probes the chemical doping state of MoS₂ and possible Cu contamination on the surface of MoS₂ after transfer. The Mo 3d spectrum (**Figure 5a**) and S 2p spectrum (**Figure S3a**) of as-grown MoS₂/EG and transferred MoS₂/SiO₂ both show evidence of pristine MoS₂, suggesting that the MoS₂ retains its chemical state following transfer.¹³ The Cu spectrum shown in **Figure S3b** also shows no detectable Cu impurities on the surface of transferred MoS₂/SiO₂.

Raman spectroscopy is also useful for characterizing graphene and MoS₂, providing insight into layer number, strain, and doping.^{37,41,42} While both samples show the out-of-plane A_{1g} and the in-plane E_{12g} modes associated with MoS₂, the transferred MoS₂ sample shows no G and 2D band peaks belonging to graphene (**Figure 5b**). The difference between the E_{12g} and A_{1g} Raman modes is ~20 cm⁻¹ on both samples, which corresponds to monolayer MoS₂.^{11,43} The negligibly shifted E_{12g} mode also presents no obvious change in the strain state of MoS₂ before and after transfer.⁴⁴⁻⁴⁶ In contrast, the A_{1g} mode of transferred MoS₂/SiO₂ is redshifted by ~2.6 cm⁻¹. This shift is likely due to the different dielectric environments between graphene and SiO₂, rather than a doping effect from the processing solutions (**Figure S4**).⁴¹ **Figure 5c** further shows the normalized PL spectra of as-grown MoS₂/EG and transferred MoS₂/SiO₂. The PL intensity of the transferred MoS₂ sample is increased by ~10-fold compared to as-grown MoS₂/EG, which is in agreement

with the known PL quenching of MoS₂ by graphene.⁴⁷ Spatial mapping of the PL intensity before and after transfer verifies this result over large areas (**Figure S5**). Moreover, the PL peak position of transferred MoS₂/SiO₂ is blue-shifted by ~16 nm. This shift likely originates from the change of strain state in MoS₂. The transfer of as-grown MoS₂/SiO₂ shows similar results (**Figure S4d**).^{48,49}

To investigate the electrical properties of the transferred MoS₂ crystals, field-effect transistors (FETs) were fabricated using electron-beam lithography and electron-beam deposition. **Figure 6a** shows the output characteristics for a MoS₂-FET measured in a vacuum probe station at a pressure of < 2 × 10⁻⁵ Torr at room temperature. The source-drain current changes linearly with source-drain voltage for a given gate voltage, demonstrating nearly Ohmic contacts.⁵⁰

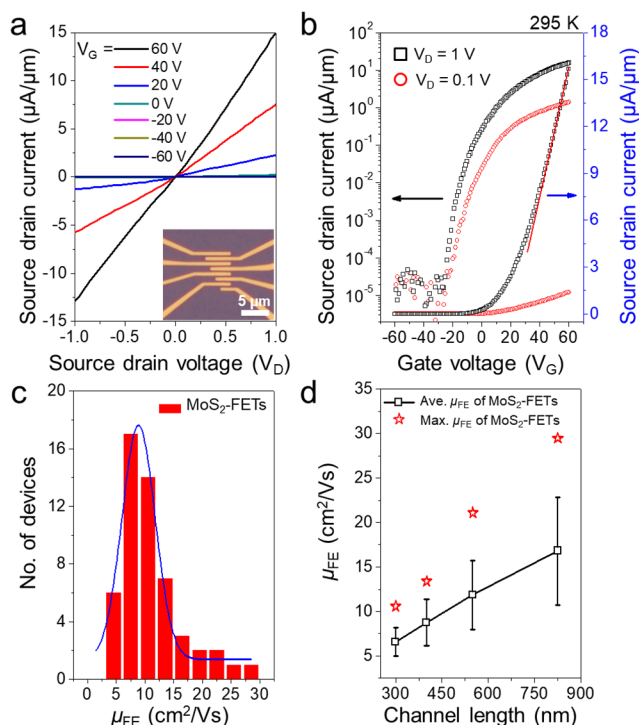


Figure 6. Electrical characterization of transferred MoS₂. (a) Output and (b) transfer characteristics of a MoS₂-FET. Inset is the optical image of the MoS₂-FET. (c) Statistics for MoS₂-FET field-effect mobility. (d) Average and maximum values of the field-effect mobility for MoS₂-FETs with different channel lengths.

Figure 6b contains representative linear and semi-logarithmic transfer curves of a MoS₂-FET, showing n-type behavior with a current on/off ratio of $\sim 10^6$. The field-effect mobility (μ_{FE}) of the MoS₂-FETs can be extracted from the following equation: $\mu = (1/C_i) \times (d\sigma/dV_G)$, where C_i is the capacitance of 300 nm SiO₂ (1.1×10^{-8} Fcm⁻²), σ is the conductivity of MoS₂, and V_G is the applied gate voltage. The μ_{FE} for this device is calculated to be ~ 30 cm²/V·s at 1 V, which is comparable to the values from previous reports for monolayer MoS₂ grown by CVD.⁵¹⁻⁵³ A large array of devices with different channel lengths enables statistical assessment of the spatial uniformity of the transferred MoS₂ electrical properties (**Figure S6**). In order to fabricate MoS₂ devices with different channel lengths from 300 nm to 1000 nm, we used MoS₂ single domains for small channel lengths under 500 nm and a merged MoS₂ domain for large channel lengths over 500 nm. A histogram of the extracted μ_{FE} from 54 devices is provided in **Figure 6c**. **Figure S7** further shows the distributions of μ_{FE} at different channel lengths with a total of 12-14 devices measured for each channel length. The resulting average and maximum μ_{FE} values are plotted as function of channel length in **Figure 6d**. The average values and standard deviations of μ_{FE} are 6.6 ± 1.6 , 8.8 ± 2.6 , 11.9 ± 3.9 , and 16.8 ± 6.0 cm²/V·s for 300 nm, 400 nm, 550 nm, and 825 nm channel lengths, respectively. These values are quantitatively comparable to μ_{FE} values at each channel length for CVD MoS₂ grown on SiO₂.⁵² Therefore, these results confirm that our transfer technique retains the intrinsic electrical properties of CVD MoS₂.

CONCLUSIONS In summary, following DFT predictions of binding energies in MoS₂-based heterostructures, high quality monolayer MoS₂ was successfully transferred from EG/SiC substrates to SiO₂/Si substrates using Cu adhesion layers. AFM and SEM images show that the transfer process retains the rotational ordering of the MoS₂ crystals, while TEM and SAED confirm high MoS₂ crystallinity following transfer. This microscopic characterization coupled with XPS shows that the transferred MoS₂ flakes are also free from defects, wrinkles, and residues. As evidenced by Raman and PL measurements, the transfer process selectively and cleanly transfers MoS₂ and enhances the MoS₂ PL intensity in comparison to MoS₂ on EG. High electrical performance of transferred MoS₂-FETs also show that this transfer process preserves the intrinsic electrical properties of CVD MoS₂. Overall, this study represents a technical advance in clean 2D materials transfer over large-scales with high-fidelity that enables further studies of the intrinsic optical and electronic properties of TMDs grown *via* van der Waals epitaxy. Furthermore, our methodology of using DFT to screen adhesion layers will inform future transfer efforts aimed at emerging 2D materials beyond graphene and TMDs.

ASSOCIATED CONTENT

Supporting Information. The Supporting Information is available free of charge on the ACS Publications website, and includes additional AFM, Raman, PL, XPS, and electrical characterization in addition to details on the DFT methodology.

AUTHOR INFORMATION

Corresponding Author

*E-mail: m-hersam@northwestern.edu

Present Addresses

†Robert Bosch LLC, Research and Technology Center, Cambridge, Massachusetts 02139, United States.

Author Contributions

‡J. Kang and I. Balla contributed equally.

Notes

The authors declare no competing financial interest.

ACKNOWLEDGMENT

This work was primarily supported by the National Science Foundation (NSF) Materials Research Science and Engineering Center (MRSEC) of Northwestern University (NSF DMR-1720139). CVD growth was supported by the National Institute of Standards and Technology (NIST ChiMaD 70NANB14H012). Raman instrumentation was funded by the Argonne-Northwestern Solar Energy Research (ANSER) Energy Frontier Research Center (DOE DE-SC0001059). This work made use of the facilities in the Northwestern University NUANCE Center, which has received support from the Soft and Hybrid Nanotechnology Experimental (SHyNE) Resource (NSF ECCS-1542205); the MRSEC program (NSF DMR-1720139) at the Materials Research Center; the International Institute for Nanotechnology (IIN); the Keck Foundation; and the State of Illinois. S.K. and C.W. were supported by the financial assistance award 70NANB14H012 from the U.S. Department of Commerce, National Institute of Standards and Technology as part of the Center for Hierarchical Materials Design (ChiMaD). This research was also supported in part through the computational resources and staff contributions of the Quest High Performance Computing Facility at Northwestern University, which is jointly supported by the Office of the Provost, the Office for Research, and Northwestern University Information Technology.

REFERENCES

- (1) Geim, A. K.; Grigorieva, I. V. van der Waals Heterostructures. *Nature* **2013**, *499*, 419-425.
- (2) Akinwande, D.; Petrone, N.; Hone, J. Two-Dimensional Flexible Nanoelectronics. *Nat. Commun.* **2014**, *5*, 5678.
- (3) Manzeli, S.; Ovchinnikov, D.; Pasquier, D.; Yazyev, O. V.; Kis, A. 2D Transition Metal Dichalcogenides. *Nat. Rev. Mater.* **2017**, *2*, 17033.
- (4) Lim, H.; Yoon, S. I.; Kim, G.; Jang, A. R.; Shin, H. S., Stacking of Two-Dimensional Materials in Lateral and Vertical Directions. *Chem. Mater.* **2014**, *26*, 4891-4903.
- (5) Kang, J.; Jariwala, D.; Ryder, C. R.; Wells, S. A.; Choi, Y.; Hwang, E.; Cho, J. H.; Marks, T. J.; Hersam, M. C. Probing Out-of-Plane Charge Transport in Black Phosphorus with Graphene-Contacted Vertical Field-Effect Transistors. *Nano Lett.* **2016**, *16*, 2580-2585.
- (6) Radisavljevic, B.; Radenovic, A.; Brivio, J.; Giacometti, V.; Kis, A. Single-Layer MoS₂ Transistors. *Nat. Nanotechnol.* **2011**, *6*, 147-150.
- (7) Lopez-Sanchez, O.; Lembke, D.; Kayci, M.; Radenovic, A.; Kis, A. Ultrasensitive Photodetectors Based on Monolayer MoS₂. *Nat. Nanotechnol.* **2013**, *8*, 497-501.
- (8) Lee, Y.; Kim, H.; Lee, J.; Yu, S. H.; Hwang, E.; Lee, C.; Ahn, J.-H.; Cho, J. H. Enhanced Raman Scattering of Rhodamine 6G Films on Two-Dimensional Transition Metal Dichalcogenides Correlated to Photoinduced Charge Transfer. *Chem. Mater.* **2016**, *28*, 180-187.
- (9) Lee, Y.-H.; Zhang, X.-Q.; Zhang, W.; Chang, M.-T.; Lin, C.-T.; Chang, K.-D.; Yu, Y.-C.; Wang, J. T.-W.; Chang, C.-S.; Li, L.-J.; Lin, T.-

W. Synthesis of Large-Area MoS₂ Atomic Layers with Chemical Vapor Deposition. *Adv. Mater.* **2012**, *24*, 2320-2325.

(10) Zhan, Y.; Liu, Z.; Najmaei, S.; Ajayan, P. M.; Lou, J. Large-Area Vapor-Phase Growth and Characterization of MoS₂ Atomic Layers on a SiO₂ Substrate. *Small* **2012**, *8*, 966-971.

(11) Wang, S.; Rong, Y.; Fan, Y.; Pacios, M.; Bhaskaran, H.; He, K.; Warner, J. H. Shape Evolution of Monolayer MoS₂ Crystals Grown by Chemical Vapor Deposition. *Chem. Mater.* **2014**, *26*, 6371-6379.

(12) Kalanyan, B.; Kimes, W. A.; Beams, R.; Stranick, S. J.; Garratt, E.; Kalish, I.; Davydov, A. V.; Kanjolia, R. K.; Maslar, J. E. Rapid Wafer-Scale Growth of Polycrystalline 2H-MoS₂ by Pulsed Metal-Organic Chemical Vapor Deposition. *Chem. Mater.* **2017**, *29*, 6279-6288.

(13) Bergeron, H.; Sangwan, V. K.; McMorro, J. J.; Campbell, G. P.; Balla, I.; Liu, X.; Bedzyk, M. J.; Marks, T. J.; Hersam, M. C. Chemical Vapor Deposition of Monolayer MoS₂ Directly on Ultrathin Al₂O₃ for Low-Power Electronics. *Appl. Phys. Lett.* **2017**, *110*, 053101.

(14) van der Zande, A. M.; Huang, P. Y.; Chenet, D. A.; Berkelbach, T. C.; You, Y.; Lee, G.-H.; Heinz, T. F.; Reichman, D. R.; Muller, D. A.; Hone, J. C. Grains and Grain Boundaries in Highly Crystalline Monolayer Molybdenum Disulfide. *Nat. Mater.* **2013**, *12*, 554-561.

(15) Najmaei, S.; Amani, M.; Chin, M. L.; Liu, Z.; Birdwell, A. G.; O'Regan, T. P.; Ajayan, P. M.; Dubey, M.; Lou, J. Electrical Transport Properties of Polycrystalline Monolayer Molybdenum Disulfide. *ACS Nano* **2014**, *8*, 7930-7937.

(16) Wang, H.; Zhang, C.; Rana, F. Surface Recombination Limited Lifetimes of Photoexcited Carriers in Few-Layer Transition Metal Dichalcogenide MoS₂. *Nano Lett.* **2015**, *15*, 8204-8210.

(17) Bao, W.; Borys, N. J.; Ko, C.; Suh, J.; Fan, W.; Thron, A.; Zhang, Y.; Buyanin, A.; Zhang, N.; Cabrini, S.; Ashby, P. D.; Weber-Bargioni, A.; Tongay, S.; Aloni, S.; Ogletree, D. F.; Wu, J.; Salmeron, M. B.; Schuck, P. J. Visualizing Nanoscale Excitonic Relaxation Properties of Disordered Edges and Grain Boundaries in Monolayer Molybdenum Disulfide. *Nat. Commun.* **2015**, *6*, 7993.

(18) Dumcenco, D.; Ovchinnikov, D.; Marinov, K.; Lazić, P.; Giberitini, M.; Marzari, N.; Sanchez, O. L.; Kung, Y.-C.; Krasnozhan, D.; Chen, M.-W.; Bertolazzi, S.; Gillet, P.; Fontcuberta i Morral, A.; Radenovic, A.; Kis, A. Large-Area Epitaxial Monolayer MoS₂. *ACS Nano* **2015**, *9*, 4611-4620.

(19) Liu, X.; Balla, I.; Bergeron, H.; Campbell, G. P.; Bedzyk, M. J.; Hersam, M. C. Rotationally Commensurate Growth of MoS₂ on Epitaxial Graphene. *ACS Nano* **2016**, *10*, 1067-1075.

(20) Liu, X.; Balla, I.; Bergeron, H.; Hersam, M. C. Point Defects and Grain Boundaries in Rotationally Commensurate MoS₂ on Epitaxial Graphene. *J. Phys. Chem. C* **2016**, *120*, 20798-20805.

(21) Reina, A.; Jia, X.; Ho, J.; Nezich, D.; Son, H.; Bulovic, V.; Dresselhaus, M. S.; Kong, J. Large Area, Few-Layer Graphene Films on Arbitrary Substrates by Chemical Vapor Deposition. *Nano Lett.* **2009**, *9*, 30-35.

(22) Li, X.; Zhu, Y.; Cai, W.; Borysiak, M.; Han, B.; Chen, D.; Piner, R. D.; Colombo, L.; Ruoff, R. S. Transfer of Large-Area Graphene Films for High-Performance Transparent Conductive Electrodes. *Nano Lett.* **2009**, *9*, 4359-4363.

(23) Kang, J.; Shin, D.; Bae, S.; Hong, B. H. Graphene Transfer: Key for Applications. *Nanoscale* **2012**, *4*, 5527-5537.

(24) Pirkle, A.; Chan, J.; Venugopal, A.; Hinojos, D.; Magnuson, C. W.; McDonnell, S.; Colombo, L.; Vogel, E. M.; Ruoff, R. S.; Wallace, R. M. The Effect of Chemical Residues on the Physical and Electrical Properties of Chemical Vapor Deposited Graphene Transferred to SiO₂. *Appl. Phys. Lett.* **2011**, *99*, 122108.

(25) Kim, J.; Bayram, C.; Park, H.; Cheng, C.-W.; Dimitrakopoulos, C.; Ott, J. A.; Reuter, K. B.; Bedell, S. W.; Sadana, D. K. Principle of Direct van der Waals Epitaxy of Single-Crystalline Films on Epitaxial Graphene. *Nat. Commun.* **2014**, *5*, 4836.

(26) Kim, Y.; Cruz, S. S.; Lee, K.; Alawode, B. O.; Choi, C.; Song, Y.; Johnson, J. M.; Heidelberger, C.; Kong, W.; Choi, S.; Qiao, K.; Almansouri, I.; Fitzgerald, E. A.; Kong, J.; Kolpak, A. M.; Hwang, J.; Kim, J. Remote Epitaxy through Graphene enables Two-Dimensional Material-Based Layer Transfer. *Nature* **2017**, *544*, 340-343.

(27) Kim, J.; Park, H.; Hannon, J. B.; Bedell, S. W.; Fogel, K.; Sadana, D. K.; Dimitrakopoulos, C. Layer-Resolved Graphene Transfer via Engineered Strain Layers. *Science* **2013**, *342*, 833-836.

(28) Zhiping, X.; Markus, J. B. Interface Structure and Mechanics between Graphene and Metal Substrates: a First-Principles Study. *J. Phys.: Condens. Matter* **2010**, *22*, 485301.

(29) Zhong, H.; Quhe, R.; Wang, Y.; Ni, Z.; Ye, M.; Song, Z.; Pan, Y.; Yang, J.; Yang, L.; Lei, M.; Shi, J.; Lu, J. Interfacial Properties of Monolayer and Bilayer MoS₂ Contacts with Metals: Beyond the Energy Band Calculations. *Sci. Rep.* **2016**, *6*, 21786.

(30) Klimeš, J.; Bowler, D. R.; Michaelides, A. M. Chemical Accuracy for the van der Waals Density Functional. *J. Phys.: Condens. Matter* **2010**, *22*, 022201.

(31) Klimeš, J.; Bowler, D. R.; Michaelides, A. van der Waals Density Functionals Applied to Solids. *Phys. Rev. B* **2011**, *83*, 195131.

(32) Aykol, M.; Kim, S.; Wolverton, C. van der Waals Interactions in Layered Lithium Cobalt Oxides. *J. Phys. Chem. C* **2015**, *119*, 19053-19058.

(33) Kim, S.; Noh, J.-K.; Aykol, M.; Lu, Z.; Kim, H.; Choi, W.; Kim, C.; Chung, K. Y.; Wolverton, C.; Cho, B.-W. Layered-Layered-Spinel Cathode Materials Prepared by a High-Energy Ball-Milling Process for Lithium-ion Batteries. *ACS Appl. Mater. Interfaces* **2016**, *8*, 363-370.

(34) Gim, Y. S.; Lee, Y.; Kim, S.; Hao, S.; Kang, M. S.; Yoo, W. J.; Kim, H.; Wolverton, C.; Cho, J. H. Organic Dye Graphene Hybrid Structures with Spectral Color Selectivity. *Adv. Funct. Mater.* **2016**, *26*, 6593-6600.

(35) Chen, K.-S.; Xu, R.; Luu, N. S.; Secor, E. B.; Hamamoto, K.; Li, Q.; Kim, S.; Sangwan, V. K.; Balla, I.; Guiney, L. M.; Seo, J.-W. T.; Yu, X.; Liu, W.; Wu, J.; Wolverton, C.; Dravid, V. P.; Barnett, S. A.; Lu, J.; Amine, K.; Hersam, M. C. Comprehensive Enhancement of Nanostructured Lithium-Ion Battery Cathode Materials via Conformational Graphene Dispersion. *Nano Lett.* **2017**, *17*, 2539-2546.

(36) Ni, G.-X.; Zheng, Y.; Bae, S.; Kim, H. R.; Pachoud, A.; Kim, Y. S.; Tan, C.-L.; Im, D.; Ahn, J.-H.; Hong, B. H.; Özyilmaz, B. Quasi-Periodic Nanoripples in Graphene Grown by Chemical Vapor Deposition and Its Impact on Charge Transport. *ACS Nano* **2012**, *6*, 1158-1164.

(37) Ferrari, A. C.; Meyer, J. C.; Scardaci, V.; Casiraghi, C.; Lazzeri, M.; Mauri, F.; Piscanec, S.; Jiang, D.; Novoselov, K. S.; Roth, S.; Geim, A. K. Raman Spectrum of Graphene and Graphene Layers. *Phys. Rev. Lett.* **2006**, *97*, 187401.

(38) Ni, Z. H.; Yu, T.; Lu, Y. H.; Wang, Y. Y.; Feng, Y. P.; Shen, Z. X. Uniaxial Strain on Graphene: Raman Spectroscopy Study and Band-Gap Opening. *ACS Nano* **2008**, *2*, 2301-2305.

(39) Mohiuddin, T. M. G.; Lombardo, A.; Nair, R. R.; Bonetti, A.; Savini, G.; Jalil, R.; Bonini, N.; Basko, D. M.; Galiotis, C.; Marzari, N.; Novoselov, K. S.; Geim, A. K.; Ferrari, A. C. Uniaxial Strain in Graphene by Raman Spectroscopy: G peak splitting, Grüneisen Parameters, and Sample Orientation. *Phys. Rev. B* **2009**, *79*, 205433.

(40) Lu, Z.; Sun, L.; Xu, G.; Zheng, J.; Zhang, Q.; Wang, J.; Jiao, L. Universal Transfer and Stacking of Chemical Vapor Deposition Grown Two-Dimensional Atomic Layers with Water-Soluble Polymer Mediator. *ACS Nano* **2016**, *10*, 5237-5242.

(41) Buscema, M.; Steele, G. A.; van der Zant, H. S. J.; Castellanos-Gomez, A. The Effect of the Substrate on the Raman and Photoluminescence Emission of Single-Layer MoS₂. *Nano Res.* **2014**, *7*, 561-571.

(42) Lee, C.; Yan, H.; Brus, L. E.; Heinz, T. F.; Hone, J.; Ryu, S. Anomalous Lattice Vibrations of Single- and Few-Layer MoS₂. *ACS Nano* **2010**, *4*, 2695-2700.

- (43) Li, H.; Zhang, Q.; Yap, C. C. R.; Tay, B. K.; Edwin, T. H. T.; Olivier, A.; Baillargeat, D. From Bulk to Monolayer MoS₂: Evolution of Raman Scattering. *Adv. Funct. Mater.* **2012**, *22*, 1385-1390.
- (44) Hui, Y. Y.; Liu, X.; Jie, W.; Chan, N. Y.; Hao, J.; Hsu, Y.-T.; Li, L.-J.; Guo, W.; Lau, S. P. Exceptional Tunability of Band Energy in a Compressively Strained Trilayer MoS₂ Sheet. *ACS Nano* **2013**, *7*, 7126-7131.
- (45) Rice, C.; Young, R. J.; Zan, R.; Bangert, U.; Wolverson, D.; Georgiou, T.; Jalil, R.; Novoselov, K. S. Raman-Scattering Measurements and First-Principles Calculations of Strain-Induced Phonon Shifts in Monolayer MoS₂. *Phys. Rev. B* **2013**, *87*, 081307.
- (46) Castellanos-Gomez, A.; Roldán, R.; Cappelluti, E.; Buscema, M.; Guinea, F.; van der Zant, H. S. J.; Steele, G. A. Local Strain Engineering in Atomically Thin MoS₂. *Nano Lett.* **2013**, *13*, 5361-5366.
- (47) Ago, H.; Endo, H.; Solís-Fernández, P.; Takizawa, R.; Ohta, Y.; Fujita, Y.; Yamamoto, K.; Tsuji, M. Controlled van der Waals Epitaxy of Monolayer MoS₂ Triangular Domains on Graphene. *ACS Appl. Mater. Interfaces* **2015**, *7*, 5265-5273.
- (48) Liu, K.; Yan, Q.; Chen, M.; Fan, W.; Sun, Y.; Suh, J.; Fu, D.; Lee, S.; Zhou, J.; Tongay, S.; Ji, J.; Neaton, J. B.; Wu, J. Elastic Properties of Chemical-Vapor-Deposited Monolayer MoS₂, WS₂, and Their Bilayer Heterostructures. *Nano Lett.* **2014**, *14*, 5097-5103.
- (49) Pierucci, D.; Henck, H.; Naylor, C. H.; Sediri, H.; Lhuillier, E.; Balan, A.; Rault, J. E.; Dappe, Y. J.; Bertran, F.; Fèvre, P. L.; Johnson, A. T. C.; Ouerghi, A. Large Area Molybdenum Disulphide-Epitaxial Graphene Vertical van der Waals Heterostructures. *Sci. Rep.* **2016**, *6*, 26656.
- (50) Jariwala, D.; Sangwan, V. K.; Late, D. J.; Johns, J. E.; Dravid, V. P.; Marks, T. J.; Lauhon, L. J.; Hersam, M. C. Band-Like Transport in High Mobility Unencapsulated Single-Layer MoS₂ Transistors. *Appl. Phys. Lett.* **2013**, *102*, 173107.
- (51) Kang, K.; Xie, S.; Huang, L.; Han, Y.; Huang, P. Y.; Mak, K. F.; Kim, C.-J.; Muller, D.; Park, J. High-Mobility Three-Atom-Thick Semiconducting Films with Wafer-Scale Homogeneity. *Nature* **2015**, *520*, 656-660.
- (52) Liu, H.; Si, M.; Najmaei, S.; Neal, A. T.; Du, Y.; Ajayan, P. M.; Lou, J.; Ye, P. D. Statistical Study of Deep Submicron Dual-Gated Field-Effect Transistors on Monolayer Chemical Vapor Deposition Molybdenum Disulfide Films. *Nano Lett.* **2013**, *13*, 2640-2646.
- (53) Schmidt, H.; Giustiniano, F.; Eda, G. Electronic Transport Properties of Transition Metal Dichalcogenide Field-Effect Devices: Surface and Interface Effects. *Chem. Soc. Rev.* **2015**, *44*, 7715-7736.

TOC image

